Cancer Immunol Immunother (2010) 59:367–378
DOI 10.1007/s00262-009-0755-y

ORIGINAL ARTICLE

Chronic bacterial osteomyelitis suppression of tumor growth requires innate immune responses

Joseph L. Sottnik · Lance W. U'Ren · Douglas H. Thamm · Stephen J. Withrow · Steven W. Dow

Received: 11 March 2009 / Accepted: 4 August 2009 / Published online: 23 August 2009

Abstract Clinical studies over the past several years have reported that metastasis-free survival times in humans and dogs with osteosarcoma are significantly increased in patients that develop chronic bacterial osteomyelitis at their surgical site. However, the immunological mechanism by which osteomyelitis may suppress tumor growth has not been investigated. Therefore, we used a mouse model of osteomyelitis to assess the effects of bone infection on innate immunity and tumor growth. A chronic Staphylococcal osteomyelitis model was established in C3H mice and the effects of infection on tumor growth of syngeneic DLM8 osteosarcoma were assessed. The effects of infection on tumor angiogenesis and innate immunity, including NK cell and monocyte responses, were assessed. We found that osteomyelitis significantly inhibited the growth of tumors in mice, and that the effect was independent of the infecting bacterial type, tumor type, or mouse strain. Depletion of NK cells or monocytes reversed the antitumor activity elicited by infection. Moreover, infected mice had a significant increase in circulating monocytes and numbers of tumor associated macrophages. Infection suppressed tumor angiogenesis but did not affect the numbers of circulating endothelial cells. Therefore, we concluded that chronic localized bacterial infection could elicit significant systemic antitumor activity dependent on NK cells and macrophages.

J. L. Sottnik · D. H. Thamm · S. J. Withrow · S. W. Dow (✉)
Department of Clinical Sciences, Animal Cancer Center, Colorado State University, Ft. Collins, CO 80523, USA
e-mail: sdow@colostate.edu

J. L. Sottnik
e-mail: jsottnik@rams.colostate.edu

L. W. U'Ren · S. W. Dow
Department of Microbiology, Immunology, and Pathology, Animal Cancer Center, Colorado State University, Ft. Collins, CO 80523, USA

Keywords Inflammation · Osteosarcoma · Innate immunity

Introduction

The ability of bacterial infections to inhibit tumor growth was first described over a century ago by Dr. Coley [1]. Coley suggested that the fever accompanying the infection led to a warming of the tumor which triggered tumor regression [2]. More recent studies have shown that systemic infection with non-bacterial pathogens is capable of inhibiting tumor growth. For example, infection with *Toxoplasma gondii* has been shown to suppress tumor growth via induction of IFN-γ release and suppression of tumor angiogenesis leukocyte recruitment [3, 4].

Models of tumor localized infection, where bacteria home directly to the tumor, have been used as one approach for tumor immunotherapy [5–8]. The homing of the pathogen to the tumor triggers leukocyte recruitment to tumor tissues, which is believed to stimulate non-specific antitumor immunity. Genetically altered bacteria and viruses have also been used to deliver immunostimulatory cytokines and other anti-tumor molecules to the tumor microenvironment [6, 7, 9–13]. Studies in various tumor models have shown that these approaches elicit leukocyte recruitment to the tumor and promote anti-tumor activity.

Osteosarcoma is the most common primary bone tumor in humans and dogs, and the tumor in dogs is widely viewed as the most relevant animal model for human osteosarcoma [14, 15]. Tumor metastasis is the most common cause of death from osteosarcoma [16]. For this reason, both humans and dogs with osteosarcoma typically receive adjuvant chemotherapy [14, 17]. Despite the use of chemotherapy, the long term survival of dogs with osteosarcoma

remains less than 30% [16]. In humans, the overall 5-year survival is 60% with surgery and adjuvant chemotherapy as the standard of care [17].

It was recently reported that dogs with osteosarcoma developing localized osteomyelitis following limb-sparing surgery had significantly increased metastasis-free intervals and survival times, compared to dogs that did not develop infections [18]. Survival times were nearly doubled in dogs that developed osteomyelitis. Even when adjusted for other confounding variables, bone infection was significantly associated with inhibition of metastasis in these dogs. Furthermore, the authors noted that disease progression and survival effects were due to the delay in metastasis, rather than to local recurrence of disease [18]. Similar findings were reported in humans with osteosarcoma that developed osteomyelitis at the site of limb-sparing surgery [19], although it should be noted that a second study in humans with osteosarcoma failed to find an association with bone infection and survival times [20]. These findings suggest that localized osteomyelitis may elicit an immune response that is associated with the inhibition of tumor growth and metastasis.

Therefore, we hypothesized that localized bacterial osteomyelitis was capable of eliciting systemic antitumor immunity. To test this hypothesis, we developed a mouse model of chronic osteomyelitis and subcutaneously implanted syngeneic DLM8 osteosarcoma cells [21]. Using this model, we found that localized bone infection could suppress tumor growth through sustained activation of innate immune responses. These findings are important because they suggest that chronic, sustained, low-level inflammation could be used therapeutically to control tumor growth.

Materials and methods

Cell lines

The mouse osteosarcoma tumor cell line, DLM8, was generously provided by Dr. Eugenie Kleinerman (MD Anderson Cancer Center) and was maintained in C/10 Dulbecco's modified Eagle media [DMEM (Lonza, Walkersville, MD, USA) supplemented with 1× MEM vitamin solution (Cellgro, Henderson, VA, USA), 2 mM L-glutamine (Cellgro), 1 mM sodium pyruvate (Cellgro), 1× non-essential amino acid solution (Cellgro), 1× antibiotic/antimycotic (Cellgro), and 10% heat inactivated fetal bovine serum (FBS, Atlas, Fort Collins, CO, USA)]. The murine CT26 (colon carcinoma) and B16 (melanoma) cell lines were maintained in C/5/5 MEM media [MEM (Lonza) and supplemented as described above with 5% FBS and 5% heat inactivated newborn calf serum (Hyclone, Logan, UT, USA)].

Bacteria

Staphylococcus aureus stably expressing both the luciferase and luciferin genes (XEN36) was purchased from Xenogen/Caliper Life Sciences (Hopkinton, MA, USA). *Pseudomonas aeruginosa* engineered to stably express luciferase and luciferin was kindly provided by Dr. Herbert Schweizer (Colorado State University). Bacteria were grown to log phase in LB Broth (USB Corporation, Cleveland, OH, USA), then bacterial stocks were tittered and frozen at −80C prior to use.

Animals

All animal studies were performed in an AALAC-approved facility, with approval of the Colorado State University Institutional Animal Care and Use Committee. Female mice 8–10 weeks of age were used for all experiments, and were purchased from Harlan Sprague–Dawley (Indianapolis, IN, USA). C3H-HeN mice were used for all experiments involving the DLM8 tumor cell line, BALB/c mice were used for all studies involving the CT26 tumor cell line, and C57BL/6 mice were used for experiments involving the B16 tumor cell line. Five mice per group were used for all in vivo experiments.

Bacterial osteomyelitis model

Osteomyelitis was induced in mice, using a modification of a previously reported technique [22]. Briefly, bacteria were cultured in sterile LB broth at 37°C in a shaking incubator for 4–6 h to log growth. Bacteria were diluted to a concentration of 1×10^6 CFU per mL in LB broth, and 3 mm segments of 3–0 braided silk suture (Syneture, Norwalk, CT, USA) were incubated in the bacteria for 2 h at 37°C on a shaking incubator. To induce biofilm formation on the suture material, suture segments were then transferred to sterile LB broth and incubated for an additional 36 h in a shaking incubator, with the culture medium changed every 12 h. Control suture segments were prepared similarly, except without bacterial infection.

Mice were anesthetized using isoflurane (Minrad, Bethlehem, PA, USA) for the procedure. A 25 g needle (Becton–Dickinson, Franklin Lakes, NJ, USA) was used to drill a perpendicular hole in the proximal tibia. The hole was then enlarged through the use of a 23 g needle (Becton–Dickinson) to facilitate insertion of the suture segment. Suture segments were placed into the medullary cavity of the tibia. Mice receiving infected and sham treated suture material received buprenorphine (0.05 mg/kg) administered subcutaneously every 12 h for 72 h post-surgery.

In vivo imaging of infected bone

The bone site of infection was evaluated 2–3 times weekly to assess the intensity of bacterial infection by quantifying luciferase expression intensity. Imaging was performed using an IVIS 100 imaging system and Living Image version 2.50.1 software (Xenogen). Mice were anesthetized with isoflurane and imaged. A 1 min exposure time with high sensitivity binning was used to enhance quantification of the infection. The minimum intensity was set at 10% of the maximum, and a contour ROI plot with default parameters (ROI edge value of 5%) chosen to increase objectivity. Total flux of the ROI was recorded as photons/s for each sample.

Determination of bacterial burden in tissues

To determine whether bacterial infection had disseminated from the site of bone infection to other tissues, mice were sacrificed at the peak of bone infection, 10 days post-infection, and blood, spleen, liver, lung, infected tibia, opposite tibia, and tumor tissue were dissociated for determination of bacterial counts (colony forming units; CFU). Tissues were subjected to collagenase digestion and trituration before serial dilutions of supernatants were plated on LB agar plates (Fisher, Fair Lawn, NJ, USA) and incubated overnight at 37°C. Bacterial colonies were counted visually and CFU per organ were determined. Plates were imaged using the IVIS system described above to identify luciferase-positive colonies and exclude contaminating organisms.

Tumor challenge and growth model

Three days after establishment of bone infection, mice were injected with 2×10^6 DLM8 tumor cells subcutaneously (s.c.) on the contralateral flank to the bone infection. In other experiments, B16 and CT26 tumor cells were injected s.c. at a concentration of 5×10^5 cells per mouse. Mice were then imaged as previously described, and tumors measured two to three times a week using calipers. Mice were tail bled weekly by lateral tail vein to assess changes in circulating cell populations by flow cytometry. All mice were euthanized when the tumor of the first mouse in the control group reached a tumor diameter of 10 mm, except in survival experiments where each mouse was sacrificed when the individual tumor reached a size of 10 mm.

NK cell depletion

NK depletion was performed by intraperitoneal (i.p.) injection of 50 μL rabbit anti-asialo GM1 antiserum (Wako Pure Chemical Industries, Inc., Osaka, Japan), as described previously [23]. Treatment was initiated 3 days post-tumor challenge and continued weekly. This treatment resulted in depletion of 73% of $NKG2D^+$ cells in the spleen (data not shown).

Macrophage depletion

Monocytes and macrophages were depleted by intravenous (i.v.) injection of liposomal clodronate, as reported previously [24–27]. Liposomal clodronate was prepared as described previously [28]. Control liposomes were prepared similarly, except that phosphate-buffered saline (PBS) was used instead of clodronate. Treatment with liposomal clodronate was initiated 3 days after tumor challenge and continued weekly. The efficiency of monocyte depletion was assessed by flow cytometry, and i.v. injection of liposomal clodronate was found to deplete 71% of circulating monocytes (Fig. 7a). Injection of PBS liposomes did not deplete monocytes (data not shown).

Flow cytometry

Leukocytes in the blood, tumor, spleen, and lymph node tissues were quantified using flow cytometry. Blood was lysed in ACK lysis buffer to remove red blood cells from analysis. Cells were then washed in FACS buffer (1× PBS with 2% FBS and 0.1% sodium azide). Tumor, spleen, and lymph node tissues were prepared by collagenase digestion and the single cell suspension were washed once in FACS buffer.

Single cell suspensions, at a concentration of 5×10^5–1×10^6 cells per well, were immunostained with the following antibodies: anti-mouse CD3-APC-alexa fluor 750 (clone 17A2), anti-mouse NKG2D-APC (clone CX5), anti-mouse CD4-PB (clone RM4-5), anti-mouse CD8-PE/Cy7 (clone 53–6.7), anti-mouse CD11b-biotin (clone M1/70), anti-mouse CD3-biotin (clone ebio500A2), anti-mouse CD31-FITC (clone 390), anti-mouse CD11b-APC/Cy7 (clone M1/70), anti-mouse CD115-PE (clone AFS98), anti-mouse F4/80-APC (clone BM8), and anti-mouse Gr-1-PE/Cy7 (clone RB6-8C5) were purchased from eBioscience (San Diego, CA, USA); anti-human CD45-Pacific Orange (clone HI30) and nuclear stain (LDS-75) were purchased from Caltag/Invitrogen (Eugene, OR, USA); and anti-mouse Ly6G-FITC (clone 1A8) and anti-mouse Ly6C (clone AL-21) were purchased from BD Pharmingen (San Jose, CA, USA). For biotinylated antibodies, streptavidin conjugates were used to provide flourophores for analysis (eBioscience and Invitrogen).

Neutrophils were defined as being $Ly6G^+CD11b^+$. Monocytes were defined as being $Ly6G^-CD11b^+CD115^+$ $Ly6C^+$ and were further subdivided into steady state ($Ly6C^{lo}$) and inflammatory ($Ly6C^{hi}$) monocytes. Macrophages were

defined as $Ly6G^{-}CD11b^{+}F4/80^{+}$. NK cells were defined as $CD3^{-}CD4^{-}CD8^{-}NKG2D^{+}$. Circulating endothelial cells were defined as $CD45^{-}CD11b^{-}CD3^{-}CD31^{+}LDS\text{-}751^{+}$. Endothelial cells in tumor tissues were identified as $CD45^{-}CD11b^{-}CD3^{-}CD31^{+}$.

Prior to immunostaining, cells were first blocked for non-specific staining using unlabelled anti-mouse Fcr III antibody (CD16/32; clone 93; eBioscience) diluted in normal mouse serum (Jackson Immunoresearch). Immunostaining was performed at room temperature for 30 min, and then the samples were washed. Spleen and lymph node samples were fixed in 1% paraformaldehyde prior to flow cytometric analysis; blood and tumor samples were not fixed but analyzed immediately. Samples were analyzed using a CyAn ADP flow cytometer (Beckman-Coulter, Fullerton, CA, USA) and analysis performed using Summit software v4.3 (Beckman-Coulter).

Immunochemistry

The following antibodies were used for immunohistochemistry: anti-mouse purified CD31 antibody (clone 390; eBioscience), anti-mouse purified CD68 antibody (clone FA-11; AbD Serotec, Raleigh, NC, USA), biotinylated donkey anti-rat (Jackson ImmunoResearch). Tumor tissues were embedded in OCT embedding medium (Sakura, Torrance, CA, USA) and cryosectioned into 4 μm sections. Slides were rehydrated, non-specific binding blocked with appropriate serum, then incubated with appropriately diluted primary antibodies. After washing, sections were incubated with appropriate biotinylated secondary antibody described above. A Vectastain ABC kit (Vector) and subsequent AEC peroxidase substrate kit (Vector) were used according to manufacturer's instructions. Slides were then counterstained with hematoxalin and crystal mount (Biomeda, Foster City, CA, USA) applied.

Immunohistochemical staining was analyzed in a randomized and blinded fashion. Microvessel density (MVD) was analyzed by manually counting the number of microvessels per 20× high power field, with five random fields counted per tumor section. Macrophage density was determined using five random fields and Carl Zeiss AxioVision Software v4.6 (Zeiss, Thornwood, NY, USA). Computerized determination of positively staining cells was performed by blanking against sections stained with an irrelevant isotype control antibody. The average number of vessels or macrophages per high power field was determined.

Assessment of tumor associated macrophage cytotoxicity

Tumor tissues from infected and control mice were removed and prepared by collagenase digestion. Single cell suspensions were prepared in sort buffer (1× PBS with 2% FBS) and TAM were immunostained using CD11b and F4/80, as described above. Cells were then sorted using a MoFlo Flow Cytometer (Beckman-Coulter). The purity of the recovered cells was determined by flow cytometry to be 85%.

The sorted TAM were admixed with DLM8 tumor cells at macrophage to tumor ratios of 1:2–1:8. The cells were incubated for 24 h and cytotoxicity was assessed using an LDH release assay, according to manufacturer's directions (Promega, Madison, WI, USA). As a positive control for macrophage cytotoxicity, thioglycolate-elicited peritoneal macrophages were used, following overnight activation with 20 ng/mL of IFNγ.

Statistical analysis

Statistical analysis was performed using Prism 5 (GraphPad Software, La Jolla, CA, USA). Tumor growth experiments with two groups were compared using a paired two-tailed Student's t test, and those with three or more groups were analyzed using repeated measures one-way ANOVA and Bonferroni post-test. Data from two groups was compared using a two-tailed Student's t test and data with three or more groups was compared using one-way ANOVA with Bonferroni post-test. Survival analysis, as described as time to a specific tumor diameter, was performed using Kaplan–Meier log-rank analysis. Comparison of monocytes over time was performed using a two-way ANOVA with Bonferroni post-test. For all analyses, p-values of less than 0.05 were considered statistically significant.

Results

Establishment of mouse model of chronic osteomyelitis

To study the effects of a localized bone infection on distant tumor growth, we first established a mouse model of chronic bacterial osteomyelitis, using a modification of an earlier protocol [22]. One of the primary modifications in our model was to establish bacterial biofilms on the suture prior to implantation in the marrow cavity of the tibia. This was done by prolonging the length of incubation in bacterial cultures, along with continuous shaking. We found that biofilm sutures led to more reliable infections with greater sustained luciferase intensity over time than did sutures prepared using the original method (data not shown). We also observed a 4-fold increased mean infection intensity at the bone site in mice receiving biofilm infected suture, compared to mice implanted with non-biofilm suture at 49 days after suture implantation (data not shown).

Luciferase expressing *S. aureus* biofilms were established on silk suture and placed in the medullary cavity of C3H-HeN mice ($n = 5$ per group). Following placement of the suture, the intensity of luciferase expression was determined in each infected mouse (Fig. 1a). With this infection model, we observed that there was a progressive increase in the intensity of bone infection, with the peak of infection developing 10 days post-challenge (Fig. 1a). The bone infection was also sustained, with live bacteria still detectable by luciferase imaging at the bone infection site over 50 days post-challenge.

We also determined whether the infection remained localized in the tibia, or whether the staphylococci became disseminated after bone infection; no signs of illness were noted during the infection. By Xenogen imaging we did not detect a luciferase signal at any sites besides the bone inoculation site (data not shown). However, to increase the sensitivity of detection, we also performed quantitative cultures of various organs from mice with infected limbs. We did not detect bacterial colonization of any tissues other than the inoculated bone at any time during the infection studies (data not shown). Therefore, we concluded that in this model, the infection remained localized to the site of infected bone.

Tumor growth is inhibited in mice with bacterial osteomyelitis

To determine whether bacterial osteomyelitis could inhibit tumor growth, *S. aureus* infected suture was placed in the tibia of C3H-HeN mice (n = 5 per group). Three days later, mice were injected with syngeneic DLM8 tumor cells on the contralateral rear flank. Tumor growth was assessed every 2–3 days using calipers. We found that mice with bacterial osteomyelitis had a significant decrease ($p < 0.02$) in tumor growth compared to uninfected control mice (Fig. 2a). However, in mice with tumors established 3 days before infection, we did not observe significant tumor growth inhibition (data not shown). Mice that were sham-infected with control suture did not have a significantly altered tumor growth compared to untreated mice with tumors only (data not shown). In addition, survival times, using time to reach 10 mm diameter as the event, were significantly increased ($p < 0.01$) in mice with osteomyelitis compared to control mice (data not shown). These results indicated that localized bacterial infection significantly inhibited the growth of tumors at distant sites. This finding was most consistent with the induction of a systemic antitumor response by the localized bone infection.

We next conducted experiments to determine whether the inhibition of tumor growth observed above was tumor type or mouse strain specific. To address these questions,

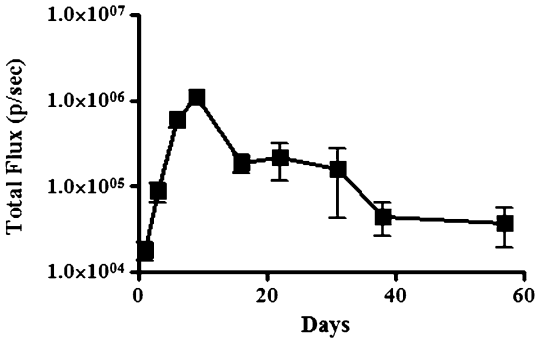

Fig. 1 *Development of localized osteomyelitis in the mouse.* Mice ($n = 5$ per group) were challenged with luciferase-transfected *Staphylococcus* biofilm-coated suture material introduced into the medullary cavity of the tibia, and imaged using a Xenogen In Vivo Imaging System to track the intensity and localization of the infection. Time course analysis of infection intensity of osteomyelitis with means (±SEM) calculated

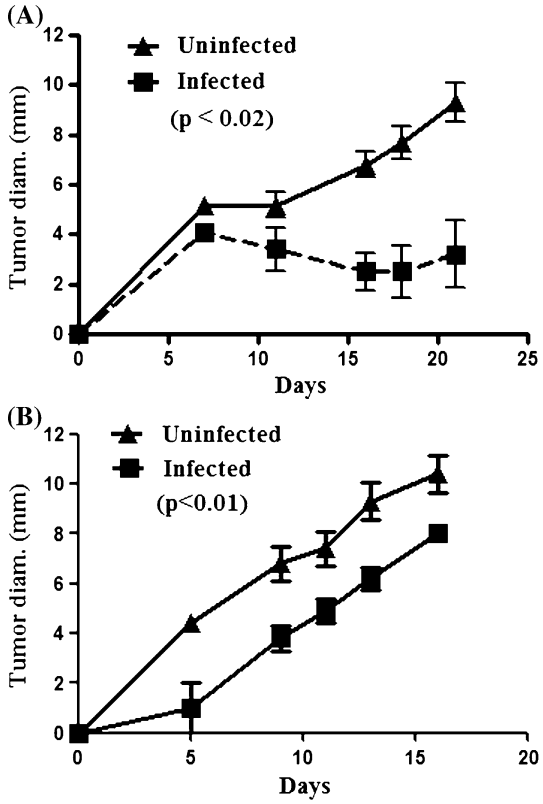

Fig. 2 *Osteomyelitis-associated tumor growth inhibition is not pathogen specific*. **a** Mice were infected with *S. aureus* containing biofilms 3 days before tumor challenge. Growth kinetics were assessed by two-dimensional measurements and the longest diameter is reported as the mean (±SEM) calculated for each group. Infected C3H mice ($n = 5$ per group) challenged with syngeneic DLM8 osteosarcoma cells have a significantly inhibited tumor growth ($p < 0.02$) compared to uninfected mice as assessed by a two-tailed paired *t* test and are representative of three independent experiments. **b** Mice were infected with *Pseudomonas aeruginosa* biofilm-impregnated suture three days prior to challenge with DLM8 cells. Tumor growth was assessed as previously described. Infected mice had a significantly ($p < 0.01$) decreased tumor growth compared to uninfected mice

we assessed the effects of osteomyelitis on tumor growth using the CT26 (colon carcinoma) model in BALB/c mice and the B16 (melanoma) model in C57BL/6 mice. In both of these models, we observed significant inhibition of tumor growth in animals with osteomyelitis compared to control animals (data not shown). Thus, we concluded that the tumor-inhibiting effects of localized osteomyelitis were not tumor type or mouse strain specific.

The preceding results indicated that chronic staphylococcal infection was capable of eliciting broad antitumor activity. However, it was possible that the antitumor activity was specific to staphylococcal infection. Therefore, osteomyelitis was induced in mice using *P. aeruginosa* instead of *S. aureus* and the effects on tumor growth were assessed. As with the staphylococcal osteomyelitis model, we observed a significant ($p < 0.01$) inhibition of tumor growth in mice with *Pseudomonas* osteomyelitis (Fig. 2b). These results suggested that inhibition of tumor growth was not specific to *Staphylococcus*, but could in fact be elicited by both gram-negative and gram-positive bacteria. Furthermore, tumor growth inhibition was independent of the effects of bacterial lipopolysaccharide (LPS), since significant inhibition was observed following staphylococcal infection.

Infection is associated with inhibition of tumor angiogenesis

Previous studies have shown that tumor angiogenesis was inhibited following infection with *T. gondii* [29]. To determine whether localized bacterial osteomyelitis was capable of inhibiting tumor angiogenesis, we assessed tumor microvessel density (MVD) in tumors from infected and control mice. Tumor sections from control and *Staphylococcus* infected mice ($n = 5$ per group) were analyzed using CD31 immunohistochemistry (Fig. 3a). We observed a significant decrease ($p < 0.01$) in tumor MVD in infected mice compared to the uninfected mice. A similar decrease in tumor $CD31^+$ endothelial cells was also noted when collagenase-digested tumor tissues were analyzed by flow cytometry (data not shown).

Recent studies indicate that tumor angiogenesis results from two independent processes; local sprouting of tumor vessels and the seeding of tumor tissues by circulating endothelial progenitor cells [30, 31]. Therefore, we used flow cytometry to assess the effects of osteomyelitis on circulating endothelial cells (CEC) in tumor-bearing mice. Using multicolor flow cytometry, we evaluated $CD45^-CD11b^-CD3^-CD31^+LDS\text{-}751^+$ CEC in the blood of tumor-bearing infected and control mice (Fig. 3b). We found no significant difference ($p > 0.05$) in CEC in infected mice with tumors compared to control mice with tumors. These results suggested that the inhibition of angiogenesis elicited by localized osteomyelitis was not mediated by suppressing the number of CEC.

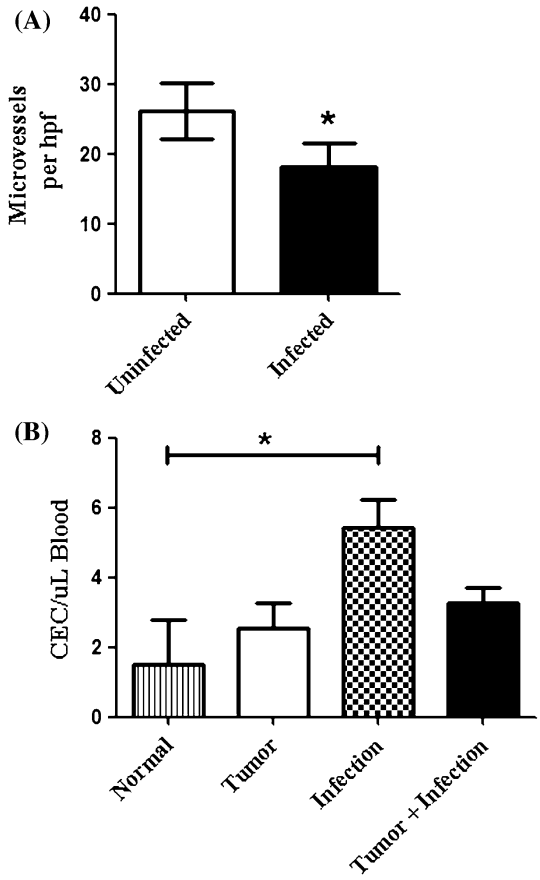

Fig. 3 *Osteomyelitis inhibits tumor angiogenesis by a CEC independent mechanism.* **a** Tumors from infected and uninfected mice were flash frozen in OCT and cut into 4 μm sections for CD31 immunohistochemistry. Microvessel density was significantly ($*p < 0.01$) decreased in the infected mice compared to the uninfected mice. Results are representative of two independent experiments. **b** CECs were assessed by flow cytometry as described in the "Materials and methods". The mean (±SEM) number of CEC per μL of blood was calculated and compared by one-way ANOVA with Bonferroni post-test. CECs from infected-tumor-bearing mice were not significantly ($p > 0.05$) different from those of tumor-bearing mice. An increase in CECs was observed in mice only challenged with infections ($*p < 0.05$), but not significantly compared to tumor only or infected mice with tumors ($p > 0.05$)

Suppression of tumor growth by infection is dependent in part on NK cells

Prior studies have shown that IFN-γ plays a prominent role in the control of tumor growth elicited by infectious agents [3, 4, 29, 32]. Since conventional NK cells are a major source of IFN-γ following bacterial and protozoal infection, we investigated the role that NK cells played in mediating tumor growth inhibition in the bacterial osteomyelitis model. To address this question, we depleted NK cells in vivo using a depleting antibody (anti-asialo GM1), as

previously reported [23]. Mice with chronic osteomyelitis were depleted of NK cells 3 days post injection of tumor cells and weekly thereafter. This treatment resulted in 73% depletion of $NKG2D^+CD3^-$ cells in the spleens of treated mice (data not shown). Tumor growth rates were compared to untreated mice with infection and uninfected tumor-bearing mice (Fig. 4). We found that NK cell depletion in infected mice with tumors led to a significant increase in tumor growth compared to untreated infected mice with tumors. However, NK depletion did not significantly alter the intensity of *Staphylococcus* infection (data not shown). Thus, NK depletion reversed the tumor inhibitory effects of chronic bone infection. In contrast, NK depletion of uninfected mice did not significantly alter tumor growth (data not shown). These results indicated that NK cells were major mediators of the inhibition of tumor growth observed following bone infection.

Chronic osteomyelitis increases inflammatory monocytes in infected mice

The preceding experiments indicated that chronic osteomyelitis activated innate immunity, as evidenced by the anti-tumor activity conferred by NK cells. Therefore, we next investigated the effects of osteomyelitis on the mobilization of monocytes in tumor-bearing mice. Previous studies have reported conflicting results for the role of monocytes in tumor growth, suggesting that they may either suppress or promote tumor growth [33, 34]. Therefore, we assessed the effects of bone infection on circulating steady state and inflammatory monocytes in the blood and spleen of mice [34–37]. Steady state monocytes were identified as $Ly6G^-CD11b^+CD115^+Ly6C^{lo}$, while inflammatory monocytes were identified as $Ly6G^-CD11b^+CD115^+Ly6C^{hi}$. Inflammatory monocytes have been found to be more likely to differentiate into activated macrophages with an anti-tumor phenotype than steady state monocytes [38, 39].

We found that total monocytes were significantly ($p < 0.05$) increased in the circulation of mice with osteomyelitis compared to uninfected mice (Fig. 5a). The numbers of steady state monocytes in the blood were not increased, whereas there was a significant ($p < 0.001$) increase in inflammatory monocytes in infected animals (Fig. 5b). A significant ($p < 0.05$) increase in the number of inflammatory monocytes in the spleen was also observed (Fig. 5c). These data are most consistent with the idea that osteomyelitis induces an inflammatory response that results in the mobilization of circulating inflammatory monocytes. This is important because these inflammatory monocytes may serve as a source of macrophages in tumor tissues.

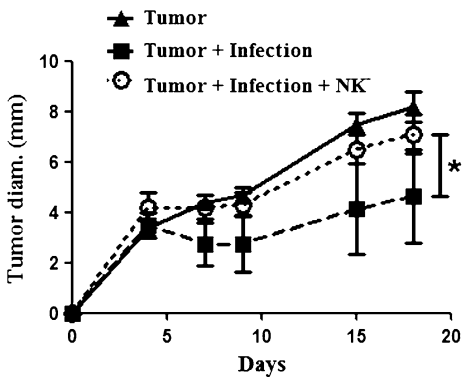

Fig. 4 *NK depletion reverses tumor growth inhibition conferred by osteomyelitis.* Mice ($n = 5$ per group) were challenged with infections and tumors as previously described. Three days after tumor challenge, mice were treated with an anti-asialo GM1 antibody administered IP to deplete NK cells, and treatment was repeated weekly. There was significant ($*p < 0.05$) growth inhibition in the infected tumor-bearing mice when compared to the uninfected mice and the NK-depleted infected mice as measure by repeated measures one-way ANOVA with Bonferroni post-test. NK-depleted infected mice did not have a significantly ($p > 0.05$) different growth when compared to tumor only mice. Results are representative of two independent experiments

Tumor associated macrophages are increased in mice with chronic osteomyelitis

Next, we examined numbers of tumor associated macrophages (TAM) and how chronic osteomyelitis affected their numbers. Though TAM are generally thought to promote tumor growth, there are situations where activated TAM may suppress tumor growth [40–42]. We used both flow cytometry and immunohistochemistry to assess numbers of TAM in tumor tissues. We found that mice ($n = 5$ per group) with osteomyelitis had twice as many $CD11b^+F4/80^+Gr\text{-}1^-$ cells in tumor tissues as uninfected mice by multi-color flow cytometry (Fig. 6a). By immunohistochemistry, we also observed a significant ($p = 0.019$) increase in $CD68^+$ TAM in mice with osteomyelitis compared to uninfected tumor-bearing mice (Fig. 6b). These findings suggested that accumulation of TAM in this chronic infection model was associated with inhibition of tumor growth.

Tumor associated macrophages are not directly cytolytic to tumor cells

To assess the cytotoxic capabilities of TAM, the TAM were sorted from tumors of uninfected and infected mice ($n = 5$ per group) and used in an in vitro cytotoxicity assay, with DLM8 tumor cells as targets. We did not observe spontaneous cytotoxic activity from either population of TAM and there was no significant ($p \geq 0.05$) difference in cytotoxicity between the two groups of mice (data not shown). As a positive control, we did note that significant anti-tumor cytotoxic activity was exerted by peritoneal exudate

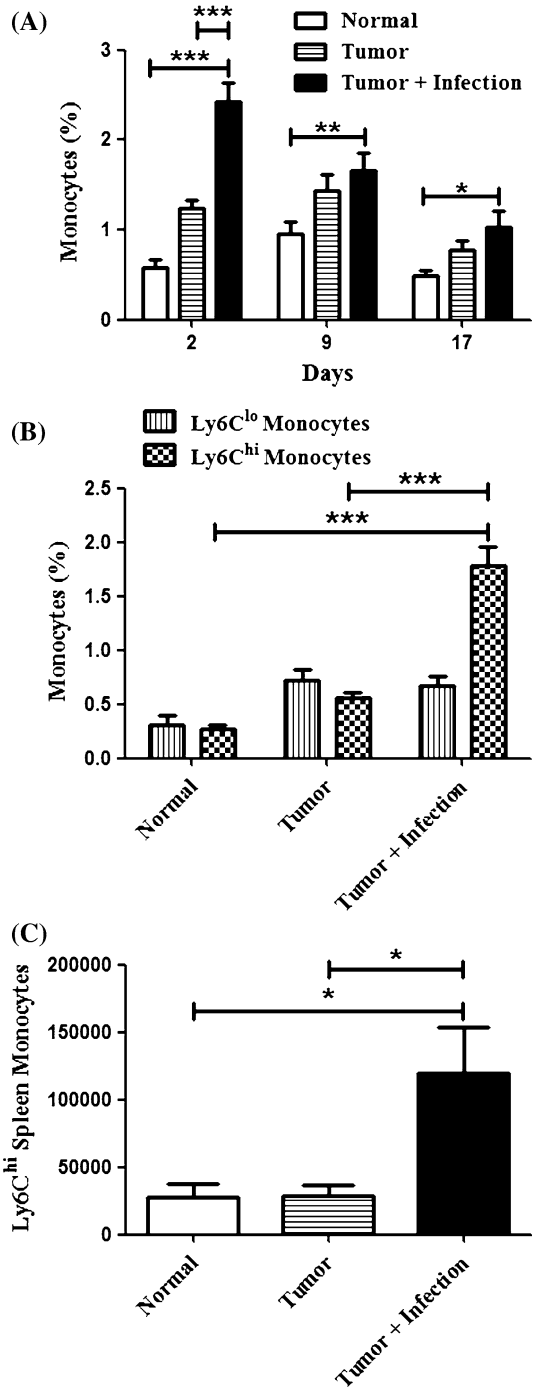

◀ **Fig. 5** *Localized osteomyelitis induces monocytes in the blood and spleen.* Mice ($n = 5$ per group) were challenged with *S. aureus* osteomyelitis and tumors as previously described. **a** Mice were tail bled on days 2, 9, and 17 post-tumor challenge. Samples were processed and analyzed by multi-color flow cytometry as described in the Materials and methods and means (±SEM) calculated for each group. There were significant (***$p < 0.001$, **$p < 0.01$, *$p < 0.05$) increases in total blood monocytes at the bracketed measures by two-way ANOVA with Bonferroni post-test. **b** Analyses from the day two bleed are further characterized showing a significant increase (***$p < 0.01$) in Ly6C^{hi} monocytes in infected mice with no difference ($p > 0.05$) in Ly6C^{lo} monocytes between groups. **c** Mice were euthanized on day 21 and spleens were analyzed by flow cytometry as described in the Materials and methods. There was a significant increase (*$p < 0.05$) in the number of Ly6C^{hi} monocytes present in the spleen measured by one-way ANOVA with Bonferroni post-test. Results are representative of three independent experiments

macrophages activated with IFN-γ (data not shown). These results therefore indicate that infection induced cytotoxic activity of TAM was unlikely to account for the tumor growth inhibition observed in the infected mice.

Monocyte and macrophage depletion reverses tumor inhibition by chronic osteomyelitis

Finally, to specifically address the antitumor role of increased inflammatory monocytes and TAM in infected mice, we conducted monocyte/macrophage depletion experiments. Depletion was accomplished by i.v. injection of liposomal clodronate (LC), which has been previously reported to efficiently deplete both monocytes and macrophages [24–26, 43]. Mice with established osteomyelitis and tumors were treated weekly with LC administered i.v. Treatment with LC resulted in a 71% depletion of blood monocytes as assessed by flow cytometry (Fig. 7a).

We observed that treatment of infected mice ($n = 5$ per group) with LC significantly increased tumor growth compared to tumors in infected mice not treated with LC (Fig. 7b). Thus, monocyte/macrophage depletion by LC appeared to reverse the antitumor effects of bone infection. In fact, tumor growth in infected mice treated with LC was similar to that of mice without infection. As a control, we found that treatment of infected tumor-bearing mice with control PBS liposomes did not have a significant impact on tumor growth compared to untreated mice with infections (data not shown). There was no significant alteration in infection intensity associated with LC treatment of infected mice (data not shown).

These results suggested that monocytes and macrophages elicited by chronic bone infection were in fact responsible for a significant degree of tumor growth inhibition. However, in a number of tumor models, we and others have observed that treatment of uninfected tumor-bearing mice with LC significantly inhibits tumor growth (Guth, AM; manuscript in preparation, [44–46]). Therefore, the results of LC depletion studies in our model suggested that substantial antitumor activity was elicited by activation of circulating inflammatory monocytes and their recruitment into tumor tissues.

Discussion

The ability of bacterial infections to suppress tumor growth was noted over a century ago by Dr. Coley and provided

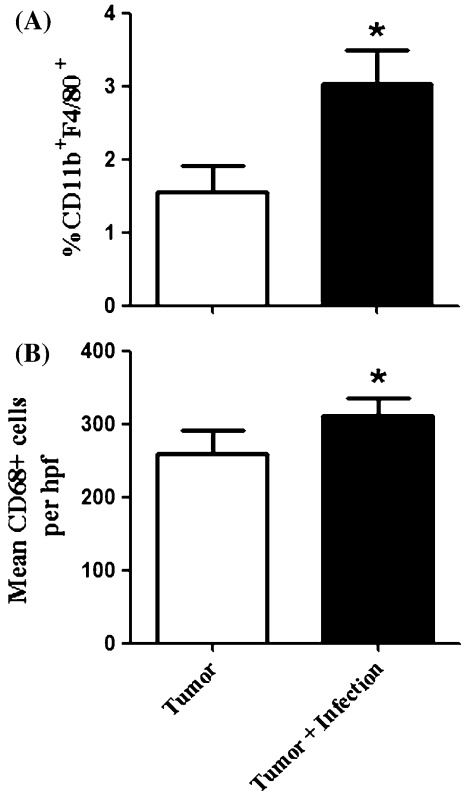

Fig. 6 *Macrophages are induced in infected, tumor-bearing mice.* Tumor-bearing mice ($n = 5$ per group) were sacrificed when the first control mouse reached a maximal tumor diameter of 10 mm. Tumors were removed and homogenized for analysis by flow cytometry or prepared for IHC as described in the Materials and methods. **a** There was a significant increase ($^*p = 0.03$) in the number of $CD11b^+F4/80^+$ macrophages in the tumors of infected mice compared to uninfected mice. **b** There was a significant increase in the number of $CD68^+$ cells per 20× high power field (hpf) in the tumor tissue of infected mice compared to the uninfected mice ($^*p = 0.019$). Results are representative of two independent experiments and two-tailed *t* tests were used to determine significance

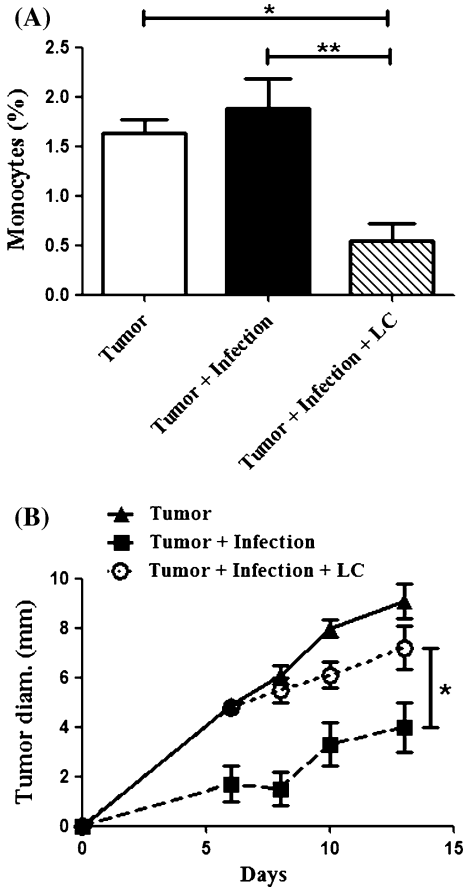

Fig. 7 *Monocyte depletion abolishes the inhibitory effects of osteomyelitis on tumor growth.* C3H mice ($n = 5$ per groups) were infected and challenged with tumors as described in the Materials and methods. Mice were administered liposomal clodronate (LC) IV 3 days after tumor challenge and then weekly thereafter. **a** Flow cytometry was performed to determine the concentration of monocytes in circulation as described in the Materials and methods. There was a significant ($^{**}p < 0.01$, $^*p < 0.05$) depletion of monocytes in the mice receiving LC compared to all other groups as determined by one-way ANOVA with Bonferroni post-test. **b** Infected mice had significantly decreased tumor growth ($^*p < 0.05$) when compared to uninfected mice and infected mice receiving LC by repeated measures one-way ANOVA with Bonferroni post-test. There was no statistical difference ($p > 0.05$) between infected mice treated with LC and uninfected tumor-bearing mice

the basis for modern day immunotherapy [1]. However, the role that systemic inflammation elicited by chronic bacterial infection plays in controlling tumor growth has yet to be well defined. Therefore, we developed a model of chronic bacterial osteomyelitis to investigate the reported ability of chronic bone infection to control the growth of osteosarcoma metastases in dogs and humans [18, 19]. Others have studied the role that localized tumor infection plays on tumor growth suppression; however, the role of systemic inflammation in mediating these tumor inhibitory effects has been incompletely described [6, 8, 47, 48].

In our infection model, we did not observe any bacterial dissemination from the site of infection, leading us to conclude that localized infection of the tumor tissues themselves did not occur. We also noted significant tumor growth inhibition in three different mouse strains, three different tumor types, and with two types of bacterial organism; suggesting that the antitumor effect was non-specific and most likely due to systemic activation of innate immune responses. However, significant growth inhibition was not observed when the tumor challenge preceded the infection. This result might be explained by the rapid and aggressive growth of the tumor lines used in these studies and the amount of time required for infection to peak following initiation.

A previous study found that systemic infection with the protozoan *T. gondii* was capable of inhibiting tumor angiogenesis [29]. In our studies, we observed tumor inhibition and decreased tumor microvessel density following the development of *Staphylococcus* osteomyelitis, the most

prominent bacterial species identified in dogs developing osteomyelitis following limb salvage surgery [18]. To better understand the nature of the anti-angiogenic effects of bone infection, we investigated the impact of infection on CEC. We observed that CEC were not decreased in tumor-bearing mice with infections, leading us to conclude that CEC changes are not likely responsible for the inhibition of angiogenesis observed by conventional CD31 staining of tumor tissues.

Previous studies have found that IFN-γ suppresses angiogenesis, and is responsible for inhibition of tumor growth in the presence of *Toxoplasma* infection [4, 29, 32, 49, 50]. Since NK cells are the major innate immune source of IFN-γ production, we depleted NK cells to identify the role these cells play in tumor inhibition. We found that depletion of NK cells reversed the protection associated with infection, indicating that NK cells were critical for inhibition of tumor growth. Others have shown that NK cell production of IFN-γ was the mechanism responsible for tumor growth control, rather than direct NK cell cytotoxicity [29]. We thus conclude that NK cells are important mediators in tumor growth control associated with osteomyelitis.

To better describe the systemic effects of infection, leukocyte changes in blood were assessed. A significant increase in inflammatory monocytes was observed in both the blood and spleen of mice with osteomyelitis. This result suggested a role for inflammatory monocytes in the inhibition of tumor growth, which the LC depletion studies confirmed. However, we cannot exclude a role for other cell types depleted by LC treatment, including macrophages and dendritic cells.

The phenotypic plasticity of monocytes and their derivatives allows them to have both pro and anti-tumor phenotypes, dependent on the stimuli present in the tumor microenvironment [40–42, 51]. We propose that increasing the number of inflammatory monocytes in circulation inhibits tumor growth by repopulating the tumor with activated TAM [24, 52, 53]. Thus, activated TAM are more likely to inhibit tumor growth than to stimulate. Furthermore, we did not observe increased direct cytolysis of tumor cells by TAM sorted from tumors of infected mice, suggesting that tumor growth inhibition was likely mediated by other macrophage activities. Other groups have shown that NK cells and monocytes can activate each other, thus leading to an activated state which may be responsible for tumor inhibition [54–56].

In conclusion, we have shown here that bacterial osteomyelitis induces significant non-specific tumor growth inhibition. The tumor growth inhibition observed following bone infection appeared to be mediated by NK cells, inflammatory monocytes, and TAM. Thus, systemic inflammation is a likely mechanism that explains the inhibition of tumor growth and metastasis observed in canine and human patients with osteosarcoma, leading to the inhibition of metastasis and increased survival in this population. It is also plausible that sustained low-level inflammation may be an important mediator of tumor growth inhibition that could be applied to the clinical management of cancer.

Acknowledgments We would like to thank Drs. Eugenie Kleinerman and Herbert Schweizer for the cell lines provided. We would like to thank Leslie Armstrong-Lea for assistance with cell sorting experiments. We would also like to thank the estate of Mr. Jeffrey Harbers for their generous donation that made this research possible.

Conflict of interest The authors declare that they have no conflict of interest.

References

1. Coley WB (1893) A preliminary note on the treatment of inoperable sarcoma by the toxic product of erysipelas. Postgrad Med 8:278–286
2. Burdick CG (1937) William Bradley Coley, 1862–1936. Ann Surg 105:152–155
3. Rankin EB, Yu D, Jiang J, Shen H, Pearce EJ, Goldschmidt MH, Levy DE, Golovkina TV, Hunter CA, Thomas-Tikhonenko A (2003) An essential role of Th1 responses and interferon gamma in infection-mediated suppression of neoplastic growth. Cancer Biol Ther 2:687–693
4. Thomas-Tikhonenko A, Hunter CA (2003) Infection and cancer: the common vein. Cytokine Growth Factor Rev 14:67–77
5. Hayashi K, Zhao M, Yamauchi K, Yamamoto N, Tsuchiya H, Tomita K, Kishimoto H, Bouvet M, Hoffman RM (2009) Systemic targeting of primary bone tumor and lung metastasis of high-grade osteosarcoma in nude mice with a tumor-selective strain of *Salmonella typhimurium*. Cell Cycle 8:870–875
6. Lee CH, Wu CL, Shiau AL (2008) *Salmonella choleraesuis* as an anticancer agent in a syngeneic model of orthotopic hepatocellular carcinoma. Int J Cancer 122:930–935
7. Ryan RM, Green J, Lewis CE (2006) Use of bacteria in anti-cancer therapies. Bioessays 28:84–94
8. Thamm DH, Kurzman ID, King I, Li Z, Sznol M, Dubielzig RR, Vail DM, MacEwen EG (2005) Systemic administration of an attenuated, tumor-targeting *Salmonella typhimurium* to dogs with spontaneous neoplasia: phase I evaluation. Clin Cancer Res 11:4827–4834
9. Kirn DH, Thorne SH (2009) Targeted and armed oncolytic poxviruses: a novel multi-mechanistic therapeutic class for cancer. Nat Rev Cancer 9:64–71
10. Loeffler M, Le'Negrate G, Krajewska M, Reed JC (2009) *Salmonella typhimurium* engineered to produce CCL21 inhibit tumor growth. Cancer Immunol Immunother 58:769–775
11. Ryan RM, Green J, Williams PJ, Tazzyman S, Hunt S, Harmey JH, Kehoe SC, Lewis CE (2009) Bacterial delivery of a novel cytolysin to hypoxic areas of solid tumors. Gene Ther 16:329–339
12. Sorenson BS, Banton KL, Frykman NL, Leonard AS, Saltzman DA (2008) Attenuated *Salmonella typhimurium* with IL-2 gene reduces pulmonary metastases in murine osteosarcoma. Clin Orthop Relat Res 466:1285–1291
13. Wei J, Wahl J, Nakamura T, Stiller D, Mertens T, Debatin KM, Beltinger C (2007) Targeted release of oncolytic measles virus by blood outgrowth endothelial cells in situ inhibits orthotopic gliomas. Gene Ther 14:1573–1586
14. Mueller F, Fuchs B, Kaser-Hotz B (2007) Comparative biology of human and canine osteosarcoma. Anticancer Res 27:155–164

15. Paoloni M, Khanna C (2008) Translation of new cancer treatments from pet dogs to humans. Nat Rev Cancer 8:147–156
16. Khanna C (2008) Novel targets with potential therapeutic applications in osteosarcoma. Curr Oncol Rep 10:350–358
17. Bielack SS, Carrle D, Hardes J, Schuck A, Paulussen M (2008) Bone tumors in adolescents and young adults. Curr Treat Options Oncol 9:67–80
18. Lascelles BD, Dernell WS, Correa MT, Lafferty M, Devitt CM, Kuntz CA, Straw RC, Withrow SJ (2005) Improved survival associated with postoperative wound infection in dogs treated with limb-salvage surgery for osteosarcoma. Ann Surg Oncol 12:1073–1083
19. Jeys LM, Grimer RJ, Carter SR, Tillman RM, Abudu A (2007) Post operative infection and increased survival in osteosarcoma patients: are they associated? Ann Surg Oncol 14:2887–2895
20. Lee JA, Kim MS, Kim DH, Lim JS, Park KD, Cho WH, Song WS, Lee SY, Jeon DG (2008) Postoperative infection and survival in osteosarcoma patients. Ann Surg Oncol 16:147–151
21. Asai T, Ueda T, Itoh K, Yoshioka K, Aoki Y, Mori S, Yoshikawa H (1998) Establishment and characterization of a murine osteosarcoma cell line (LM8) with high metastatic potential to the lung. Int J Cancer 76:418–422
22. Yoshii T, Magara S, Miyai D, Kuroki E, Nishimura H, Furudoi S, Komori T (2002) Inhibitory effect of roxithromycin on the local levels of bone-resorbing cytokines in an experimental model of murine osteomyelitis. J Antimicrob Chemother 50:289–292
23. Dow SW, Fradkin LG, Liggitt DH, Willson AP, Heath TD, Potter TA (1999) Lipid–DNA complexes induce potent activation of innate immune responses and antitumor activity when administered intravenously. J Immunol 163:1552–1561
24. Gazzaniga S, Bravo AI, Guglielmotti A, van Rooijen N, Maschi F, Vecchi A, Mantovani A, Mordoh J, Wainstok R (2007) Targeting tumor-associated macrophages and inhibition of MCP-1 reduce angiogenesis and tumor growth in a human melanoma xenograft. J Invest Dermatol 127:2031–2041
25. Huitinga I, Damoiseaux JG, van Rooijen N, Dopp EA, Dijkstra CD (1992) Liposome mediated affection of monocytes. Immunobiology 185:11–19
26. Van Rooijen N, Sanders A (1994) Liposome mediated depletion of macrophages: mechanism of action, preparation of liposomes and applications. J Immunol Methods 174:83–93
27. van Rooijen N, van Nieuwmegen R (1984) Elimination of phagocytic cells in the spleen after intravenous injection of liposome-encapsulated dichloromethylene diphosphonate. An enzyme-histochemical study. Cell Tissue Res 238:355–358
28. Mathes M, Jordan M, Dow S (2006) Evaluation of liposomal clodronate in experimental spontaneous autoimmune hemolytic anemia in dogs. Exp Hematol 34:1393–1402
29. Hunter CA, Yu D, Gee M, Ngo CV, Sevignani C, Goldschmidt M, Golovkina TV, Evans S, Lee WF, Thomas-Tikhonenko A (2001) Cutting edge: systemic inhibition of angiogenesis underlies resistance to tumors during acute toxoplasmosis. J Immunol 166:5878–5881
30. Bertolini F, Shaked Y, Mancuso P, Kerbel RS (2006) The multifaceted circulating endothelial cell in cancer: towards marker and target identification. Nat Rev Cancer 6:835–845
31. Murdoch C, Muthana M, Coffelt SB, Lewis CE (2008) The role of myeloid cells in the promotion of tumour angiogenesis. Nat Rev Cancer 8:618–631
32. Kim JO, Jung SS, Kim SY, Kim TY, Shin DW, Lee JH, Lee YH (2007) Inhibition of Lewis lung carcinoma growth by Toxoplasma gondii through induction of Th1 immune responses and inhibition of angiogenesis. J Korean Med Sci 22(Suppl):S38–S46
33. Saleh MN, Goldman SJ, LoBuglio AF, Beall AC, Sabio H, McCord MC, Minasian L, Alpaugh RK, Weiner LM, Munn DH (1995) CD16+ monocytes in patients with cancer: spontaneous elevation and pharmacologic induction by recombinant human macrophage colony-stimulating factor. Blood 85:2910–2917
34. Tacke F, Randolph GJ (2006) Migratory fate and differentiation of blood monocyte subsets. Immunobiology 211:609–618
35. Geissmann F, Jung S, Littman DR (2003) Blood monocytes consist of two principal subsets with distinct migratory properties. Immunity 19:71–82
36. Strauss-Ayali D, Conrad SM, Mosser DM (2007) Monocyte subpopulations and their differentiation patterns during infection. J Leukoc Biol 82:244–252
37. Sunderkotter C, Nikolic T, Dillon MJ, Van Rooijen N, Stehling M, Drevets DA, Leenen PJ (2004) Subpopulations of mouse blood monocytes differ in maturation stage and inflammatory response. J Immunol 172:4410–4417
38. Arnold L, Henry A, Poron F, Baba-Amer Y, van Rooijen N, Plonquet A, Gherardi RK, Chazaud B (2007) Inflammatory monocytes recruited after skeletal muscle injury switch into antiinflammatory macrophages to support myogenesis. J Exp Med 204:1057–1069
39. Varol C, Yona S, Jung S (2009) Origins and tissue-context-dependent fates of blood monocytes. Immunol Cell Biol 87:30–38
40. Lewis CE, Pollard JW (2006) Distinct role of macrophages in different tumor microenvironments. Cancer Res 66:605–612
41. Mosser DM, Edwards JP (2008) Exploring the full spectrum of macrophage activation. Nat Rev Immunol 8:958–969
42. Sica A, Allavena P, Mantovani A (2008) Cancer related inflammation: the macrophage connection. Cancer Lett 267:204–215
43. Tacke F, Ginhoux F, Jakubzick C, van Rooijen N, Merad M, Randolph GJ (2006) Immature monocytes acquire antigens from other cells in the bone marrow and present them to T cells after maturing in the periphery. J Exp Med 203:583–597
44. Hiraoka K, Zenmyo M, Watari K, Iguchi H, Fotovati A, Kimura YN, Hosoi F, Shoda T, Nagata K, Osada H, Ono M, Kuwano M (2008) Inhibition of bone and muscle metastases of lung cancer cells by a decrease in the number of monocytes/macrophages. Cancer Sci 99:1595–1602
45. Miselis NR, Wu ZJ, Van Rooijen N, Kane AB (2008) Targeting tumor-associated macrophages in an orthotopic murine model of diffuse malignant mesothelioma. Mol Cancer Ther 7:788–799
46. Zeisberger SM, Odermatt B, Marty C, Zehnder-Fjallman AH, Ballmer-Hofer K, Schwendener RA (2006) Clodronate-liposome-mediated depletion of tumour-associated macrophages: a new and highly effective antiangiogenic therapy approach. Br J Cancer 95:272–281
47. Eriksson F, Tsagozis P, Lundberg K, Parsa R, Mangsbo SM, Persson MA, Harris RA, Pisa P (2009) Tumor-specific bacteriophages induce tumor destruction through activation of tumor-associated macrophages. J Immunol 182:3105–3111
48. Homma S, Sagawa Y, Komita H, Koido S, Nagasaki E, Ryoma Y, Okamoto M (2007) Mechanism of antitumor effect on mouse hepatocellular carcinoma by intratumoral injection of OK-432, a streptococcal preparation. Cancer Immunol Immunother 56:1265–1274
49. Friesel R, Komoriya A, Maciag T (1987) Inhibition of endothelial cell proliferation by gamma-interferon. J Cell Biol 104:689–696
50. Norioka K, Borden EC, Auerbach R (1991) Inhibitory effects of cytokines on vascular endothelial cells: synergistic interactions among interferon-gamma, tumor necrosis factor-alpha, and interleukin-1. J Immunother 12:13–18
51. Mantovani A, Sozzani S, Locati M, Allavena P, Sica A (2002) Macrophage polarization: tumor-associated macrophages as a paradigm for polarized M2 mononuclear phagocytes. Trends Immunol 23:549–555
52. Dvorak HF (1986) Tumors: wounds that do not heal. Similarities between tumor stroma generation and wound healing. N Engl J Med 315:1650–1659

53. Katakura T, Miyazaki M, Kobayashi M, Herndon DN, Suzuki F (2004) CCL17 and IL-10 as effectors that enable alternatively activated macrophages to inhibit the generation of classically activated macrophages. J Immunol 172:1407–1413
54. Bluman EM, Bartynski KJ, Avalos BR, Caligiuri MA (1996) Human natural killer cells produce abundant macrophage inflammatory protein-1 alpha in response to monocyte-derived cytokines. J Clin Invest 97:2722–2727
55. Carson WE, Ross ME, Baiocchi RA, Marien MJ, Boiani N, Grabstein K, Caligiuri MA (1995) Endogenous production of interleukin 15 by activated human monocytes is critical for optimal production of interferon-gamma by natural killer cells in vitro. J Clin Invest 96:2578–2582
56. Hegde S, Chen X, Keaton JM, Reddington F, Besra GS, Gumperz JE (2007) NKT cells direct monocytes into a DC differentiation pathway. J Leukoc Biol 81:1224–1235